



## The time propagation of the stationary states of a Morse oscillator by the Gaussian wave packet method

Hansen, Flemming Yssing; Henriksen, Niels Engholm; Billing, G. D.

*Published in:*  
Journal of Chemical Physics

*Link to article, DOI:*  
[10.1063/1.455909](https://doi.org/10.1063/1.455909)

*Publication date:*  
1989

*Document Version*  
Publisher's PDF, also known as Version of record

[Link back to DTU Orbit](#)

*Citation (APA):*  
Hansen, F. Y., Henriksen, N. E., & Billing, G. D. (1989). The time propagation of the stationary states of a Morse oscillator by the Gaussian wave packet method. *Journal of Chemical Physics*, 90(6), 3060-3070.  
<https://doi.org/10.1063/1.455909>

---

### General rights

Copyright and moral rights for the publications made accessible in the public portal are retained by the authors and/or other copyright owners and it is a condition of accessing publications that users recognise and abide by the legal requirements associated with these rights.

- Users may download and print one copy of any publication from the public portal for the purpose of private study or research.
- You may not further distribute the material or use it for any profit-making activity or commercial gain
- You may freely distribute the URL identifying the publication in the public portal

If you believe that this document breaches copyright please contact us providing details, and we will remove access to the work immediately and investigate your claim.

# The time propagation of the stationary states of a Morse oscillator by the Gaussian wave packet method

F. Y. Hansen

*Fysisk-Kemisk Institut, The Technical University of Denmark, DTH 206, DK 2800 Lyngby, Denmark*

N. E. Henriksen and G. D. Billing

*Chemistry Laboratory III, H. C. Ørsted Institute, University of Copenhagen, DK 2100, Copenhagen Ø, Denmark*

(Received 13 May 1988; accepted 15 November 1988)

The Gaussian wave packet method has been developed for the simulation of processes like molecular collisions, photodissociation of molecules, and laser excitations of molecules. So far a necessary condition for an accurate result is that the fragment states are propagated accurately. We have considered one-dimensional bound states described by a Morse potential, and carried out a systematic study of the ability of the Gaussian wave packet method to propagate the stationary states. It is found that the complete set of equations of motion as derived by the minimum error method (MEM) cannot be used in practical calculations because of numerical problems. These are eliminated by the introduction of simplifications such as the independent Gaussian approximation (IGA), where each wave packet is propagated independently. The conditions for an accurate propagation within that assumption are developed, and a simple method is devised to identify those states, which are propagated accurately. This procedure may be used to investigate when the Gaussian wave packet method is appropriate for the simulation of a given process.

## I. INTRODUCTION

In the last few years new semiclassical methods, such as the Wigner method<sup>1</sup> and the Gaussian wave packet method,<sup>2</sup> have been developed for propagating quantum states in time. A common feature of the methods is that they give good well-defined results for systems with harmonic interactions. When anharmonic interactions are involved, the results often depend on the method used and disagree with exact results. The channel states or the states of the molecular fragments in collision and dissociation processes usually include bound states, which are of primary concern in this work. If the propagation of those is inaccurate the final results are poor and often ill defined,<sup>3</sup> since they, for example, may depend on the duration of the propagation. Therefore, a necessary condition for the application of a particular method to the study a given process is that the propagation of the fragment states is accurate. This condition is not sufficient for a successful calculation, however, since the interaction potential between the fragments has not been included. Thus, it will be very useful to conduct a systematic study of the ability of the various methods to give an accurate propagation of bound states determined by realistic anharmonic potentials. Since such studies have not been reported in the literature, we have studied two methods, the Gaussian wave packet method and the Wigner method. In this paper the Gaussian wave packet method is considered and in a separate paper<sup>4</sup> a similar study has been reported for the Wigner propagation method. The term "the Gaussian wave packet method" is used as a generic name for various approaches to the solution of the time-dependent Schrödinger equation all based on an expansion of the wave function in Gaussian wave packets. We have chosen to consider the bound states of the Morse potential, because it is a simple realistic repre-

sentation of the potential between two covalent bound atoms. In addition, the Morse potential is very convenient to use, because it may be specified by just one parameter  $\lambda$ , where the integer part of  $(\lambda + 0.5)$  is the number of bound states, and because relevant matrix elements may be expressed analytically.

In 1968 Chesick<sup>5</sup> suggested, in analogy to electronic energy-state calculations, the use of a real Gaussian basis set to obtain the wave functions and the energies of the stationary states of a Morse oscillator. A normalized basis set of Gaussian functions with the centers uniformly spaced along the coordinate axis were used. The widths of the Gaussian functions were all identical and chosen to be that of the ground-state harmonic-oscillator function matching the curvature of the Morse potential at the potential minimum. Earlier treatments of the problem were based on expansions in a harmonic oscillator basis set, and it was shown that the distributed Gaussian basis functions were more effective, in particular for the higher vibrational states. Shore<sup>6</sup> followed up the work of Chesick in 1973, where the numerical accuracy of the method were analyzed in further detail and compared to other methods. In particular, the effects of overcrowding were investigated. Addition of more Gaussian functions to the basis set and simultaneous reduction of the distance between adjacent functions causes a larger and larger overlap between them. This makes the overlap matrix more and more ill conditioned and inflates the numerical errors in the computations. Thus, there exists an optimal number of basis functions. The parameters of the Gaussian basis sets were restrictive and not suitable for highly anharmonic potentials. Davis and Heller<sup>7</sup> considered a generalization of the earlier treatments to a basis set of complex Gaussian functions with centers distributed throughout the phase

space. Hamilton and Light<sup>8</sup> showed in 1986 that the generalization to complex Gaussian functions is unnecessary, in cases where all eigenstates and eigenvalues are wanted to high precision. They considered a generalization of Chesick and Shore's basis set to nonuniformly spaced Gaussian functions of different widths. The centers of the Gaussians are distributed in a space limited by the turning points of the classical motion for some energy, and the centers are spaced more closely near the potential energy minimum reflecting the larger kinetic energy in that region. By relating the width of the Gaussian functions to the distance between the centers, they reduced the inaccuracies due to the overcrowding in the basis set. This more flexible basis set allows an excellent determination of the stationary states of a Morse potential with a limited number of Gaussians in the basis set.

The idea of representing a stationary wave function by a set of real Gaussian functions was extended by Heller<sup>2</sup> to the study of time-dependent quantum-mechanical processes, where the states are represented by a superposition of a set of complex Gaussian wave packets (GWP). Each function is characterized by several parameters (the position and the momentum of the packet's center, a complex width, and a complex phase) and the time evolution of those determines the wave function at time  $t$ . The equations of motion for the parameters are obtained under the assumption that the potential around the instantaneous center of each GWP may be approximated by a second order Taylor expansion of the exact potential. This approximation is referred to as the local harmonic approximation (LHA). The method was successfully applied to a variety of time-dependent processes.<sup>2,9</sup> A common feature of these applications is that they deal with the short time dynamics of localized states, where the approximations are justified.

A more general investigation of the Gaussian wave packet method has been presented by Sawada *et al.*<sup>10</sup> They explored the use of the Gaussian wave packet representation beyond the domain, where the approximations mentioned above are justified. The equations of motion are obtained by using the so-called minimum error method (MEM), which is based on a variational principle applied to the wave function itself. Basically, the equations of motion are obtained from a least-squares fit of the two terms in the time-dependent Schrödinger equation. The MEM gives the best solution to the time-dependent Schrödinger equation at any time with the given basis set. Compared to the variational principle used in the determination of the stationary states, the principle used in the MEM is much stronger, since it applies to the wave function and not only to the energy.

We have set up the MEM equations for any number of GWP and investigated the time propagation of various bound states of a series of different Morse potentials. The quality of the propagation is monitored by the norm of the state and the projection of the propagated state onto the initial state as a function of time. The former is used to test if the propagation is unitary and the latter indicates how well the state is represented by the given set of GWP, if the propagation is unitary. Although the MEM equations are exact, numerical problems tend to limit their use in practical calculations, and it is shown that the performance of approximate

methods, where no numerical problems are present, depends on how the initial set of GWP is chosen. They are chosen by the method of Hamilton and Light,<sup>8</sup> and this new approach gives a good starting point for an analysis of which states may be propagated accurately.

In the next section we discuss the Morse potential and show that it may be characterized by a single parameter  $\lambda$ . In Sec. III the MEM equations are presented and in Sec. IV the representation of the stationary states is discussed. We have supplemented the work of Hamilton and Light by a comparison of calculated and exact transition matrix elements and extended it by including a variation of the widths of the basis functions in the variational calculation. In Sec. V we analyze the numerical problems, which severely limit the practical use of the MEM. Furthermore, a series of states belonging to different Morse oscillators have been propagated using the IGA, and the results are used to deduce a criteria for which states of a given Morse oscillator may be propagated accurately using the IGA. In Sec. VI we give a summary and compare the propagation of Morse states using IGA with thawed Gaussians (as described in Sec. V) and with frozen Gaussians.

## II. THE MORSE POTENTIAL

The potential

$$v(r) = D_e \{1 - \exp[-\beta(r - r_0)]\}^2 \quad (2.1)$$

suggested by Morse<sup>12</sup> in 1929 is a useful model for the interaction between the atoms in a diatomic molecule.  $r$  is the distance between the atoms,  $D_e$  the dissociation energy of the molecule,  $\beta$  a scale factor, and  $r_0$  the equilibrium distance. The Schrödinger equation for the stationary wave functions  $\psi$  is for the problem we are considering:

$$-\frac{\hbar^2}{2\mu} \frac{\partial^2 \psi}{\partial y^2} + D_e \{1 - \exp[-\beta(y - y_0)]\}^2 \psi = E\psi, \quad (2.2)$$

where  $r$  has been replaced by  $y$  to emphasize the one-dimensional aspect.  $\mu$  is the reduced mass of the diatom and if we introduce new variables

$$x = \beta(y - y_0), \quad (2.3)$$

$$U = \frac{\hbar^2 \beta^2}{2\mu},$$

Eq. (2.2) has the form

$$-\frac{\partial^2 \psi}{\partial x^2} + \lambda^2 (1 - e^{-x})^2 \psi = \epsilon \psi \quad (2.4)$$

with

$$\lambda^2 = \frac{D_e}{U} = \frac{2\mu D_e}{\hbar^2 \beta^2}$$

and

$$\epsilon = \frac{E}{U} = \frac{2\mu E}{\hbar^2 \beta^2}. \quad (2.5)$$

Equation (2.4) shows that all systems with identical  $\lambda$  have the same set of stationary states. Analytical solutions<sup>12,13</sup> for both  $\epsilon$  and  $\Psi$  in Eq. (2.4) have been obtained, and the energies are given by

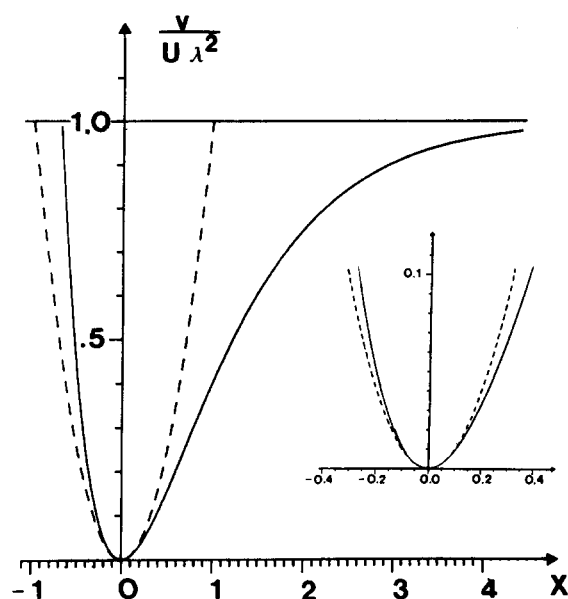


FIG. 1. A universal plot of the Morse potential  $v(x)$ . The dashed curve is the harmonic potential, which matches the potential at the minimum of the potential.  $x$ ,  $U$ ,  $\lambda$  are defined in Eqs. (2.3) and (2.5). The insert is an enlargement of the region, where anharmonic parts of the potential begin to be significant.

$$\epsilon_n = 2\lambda \left[ (n + 0.5) - \frac{1}{2\lambda} (n + 0.5)^2 \right], \quad n = 0, 1, 2, 3, \dots, (\lambda - 0.5). \quad (2.6)$$

The maximum energy of a bound state is  $\epsilon_{n_{\max}} = D_e/U$  and from Eq. (2.6) we see that  $n_{\max} = (\lambda - 0.5)$ . Thus, the number of bound states is simply given as the largest integer, which is less than or equal to  $(\lambda + 0.5)$ . Introduction of Eq. (2.3) into Eq. (2.1) gives

$$\frac{v(x)}{U} = \lambda^2 (1 - e^{-x})^2 \quad (2.7a)$$

and shows that all Morse potentials may be represented by a single graph

$$\frac{v(x)}{U\lambda^2} = (1 - e^{-x})^2. \quad (2.7b)$$

The harmonic potential, which matches the Morse potential at the energy minimum has the simple form

$$\frac{v(x)_{\text{har}}}{U\lambda^2} = x^2. \quad (2.7c)$$

The two curves [Eqs. (2.7b) and (2.7c)] are shown in Fig. 1 and may be used to give a qualitative idea of the anharmonicity of a given energy state. Herzberg<sup>14</sup> has collected the spectroscopic data for many diatomic molecules and derived the Morse potential parameters, which are given in table 39 in his book. For convenience we give the relation between  $\lambda$  and the parameters  $\omega_e$  and  $(x_e\omega_e)$  used in Herzberg's table

$$\lambda = \frac{1}{2} \frac{\omega_e}{(x_e\omega_e)}. \quad (2.8)$$

Finally, we shall give an analytical expression<sup>15</sup> for the transition matrix elements between the eigenstates of a Morse oscillator,  $\langle m|x|n \rangle$ , which in terms of the  $\lambda$  parameter is

$$\begin{aligned} \langle m|x|n \rangle &= \frac{(-1)^{n-m+1}}{(n-m)(2\lambda-n-m-1)} \\ &\quad * \left[ \frac{n!(2\lambda-n-1)!}{m!(2\lambda-m-1)!} \right. \\ &\quad \left. \times (2\lambda-2n-1)(2\lambda-2m-1) \right]^{1/2} \\ n &> m. \end{aligned} \quad (2.9)$$

This expression is used in Sec. IV to test the calculated wave functions of the Morse oscillator.

### III. THE MINIMUM ERROR METHOD AND APPROXIMATIONS

The time-dependent wave function is written as a sum of  $N$  Gaussian wave packets:

$$\begin{aligned} \Psi(x,t) &= \sum_{B=1}^N g_B(x,t), \\ g_B(x,t) &= \exp \left\{ \frac{i}{\hbar} [a_B(x - R_B)^2 + P_B(x - R_B) + \gamma_B] \right\} \\ &= \exp \left\{ -\frac{1}{\hbar} [\text{Im}(a_B)(x - R_B)^2 + \text{Im}(\gamma_B)] \right\} \exp \left\{ \frac{i}{\hbar} [\text{Re}(a_B)(x - R_B)^2 + P_B(x - R_B) + \text{Re}(\gamma_B)] \right\} \\ &= g_B[x, \xi_B(t)], \end{aligned} \quad (3.1)$$

where  $R_B$  and  $P_B$  are the average position and momentum of wave packet  $B$ . This is readily verified by forming the expectation values of the position and momentum operators.  $a_B$  and  $\gamma_B$  are the complex width and phase parameters, and  $N$  is the number of basis functions in the set.  $\xi_B(t) = [a_B(t), R_B(t), P_B(t), \gamma_B(t)]$  is a short notation for the six parameters of a wave packet with the  $j$ th member specified as  $\xi_{Bj}$ .

The wave function (3.1) is introduced in the time-dependent Schrödinger equation

$$i\hbar \frac{\partial \Psi}{\partial t} = H\Psi \quad (3.2a)$$

with the Hamiltonian  $H$  given by [see Eq. (2.4)]

$$H = -\frac{\partial^2}{\partial x^2} + \lambda^2(1 - e^{-x})^2. \quad (3.2b)$$

The equations of motion<sup>10</sup> for the  $\xi_B$  parameters are determined by first forming the sum over all points  $x$  of the squared difference between the two terms in Eq. (3.2a),

$$\sigma = \int_{-\infty}^{\infty} dx \left[ -i\hbar \sum_B \sum_j \left( \frac{\delta g_B}{\delta \xi_{Bj}} \right)^* \dot{\xi}_{Bj}^* - H \sum_B g_B^* \right] \\ * \left[ i\hbar \sum_A \sum_l \left( \frac{\delta g_A}{\delta \xi_{Al}} \right) \dot{\xi}_{Al} - H \sum_B g_B \right]$$

and then finding the minimum of  $\sigma$  with respect to all the time derivatives,  $\dot{\xi}_{Bj}$ . This gives at any time the best solution of Eq. (3.2a) with the given basis set. For the practical derivation of the equations of motion it is noted that some of the parameters,  $\xi_{Bj}$ , are complex ( $a_B, \gamma_B$ ) and some are real ( $R_B, P_B$ ). Differentiation with respect to a real parameter is straightforward, and if the parameter is complex one may choose to consider say the complex conjugate  $\xi_{Bj}^*$  as the independent variable, and we find the equations:

$\xi_{Bj}$  is a complex parameter:

$$\frac{\delta \sigma}{\delta \xi_{Bj}^*} = \int_{-\infty}^{\infty} dx \left[ \hbar^2 \left( \frac{\delta g_B}{\delta \xi_{Bj}} \right)^* \sum_A \sum_l \left( \frac{\delta g_A}{\delta \xi_{Al}} \right) \dot{\xi}_{Al} \right. \\ \left. + i\hbar \left( \frac{\delta g_B}{\delta \xi_{Bj}} \right)^* H \sum_A g_A \right] = 0, \quad (3.3a)$$

$\xi_{Bj}$  is a real parameter:

$$\frac{\delta \sigma}{\delta \xi_{Bj}} = \int_{-\infty}^{\infty} dx \left\{ \text{Re} \left[ \hbar^2 \left( \frac{\delta g_B}{\delta \xi_{Bj}} \right) \sum_A \sum_l \left( \frac{\delta g_A}{\delta \xi_{Al}} \right) \dot{\xi}_{Al}^* \right] \right. \\ \left. + \text{Re} \left[ i\hbar \left( \frac{\delta g_B}{\delta \xi_{Bj}} \right)^* H \sum_A g_A \right] \right\} = 0. \quad (3.3b)$$

Developments of the equations in (3.3) lead to the matrix equation

$$CX = V. \quad (3.4)$$

$C$  is a  $3 \times 3$  block matrix, where each block is a  $N \times N$  matrix and the elements in each block are given by

$$C = \begin{bmatrix} C(A,2;B,2) & C(A,2;B,0) & C(A,2;B,1) \\ C(A,0;B,2) & C(A,0;B,0) & C(A,0;B,1) \\ C(A,1;B,2) & C(A,1;B,0) & C(A,1;B,1) \end{bmatrix},$$

$$A, B = 1, 2, 3, \dots, N \quad (3.5a)$$

with

$$C(A,n;B,m) = \langle (x - R_A)^n (x - R_B)^m g_A^* g_B \rangle.$$

$X$  is a  $3 \times 1$  block matrix, where each block is a  $N \times 1$  matrix with the elements in each block given by

$$X = \begin{bmatrix} \dot{a}_A + 2a_A^2/\mu \\ \dot{\gamma}_A - i\hbar a_A/\mu - P_A \dot{R}_A + P_A^2/2\mu \\ \dot{P}_A + 2a_A(P_A/\mu - \dot{R}_A) \end{bmatrix}, \quad (3.5b)$$

$$A = 1, 2, 3, \dots, N.$$

$V$  is a  $3 \times 1$  block matrix, where each block is a  $N \times 1$  matrix, and the elements in each block are given by

$$V = - \frac{V(A,2;1,0) + \dots + V(A,2;N,0)}{V(A,0;1,0) + \dots + V(A,0;N,0)}, \quad (3.5c)$$

$$A = 1, 2, 3, \dots, N$$

with

$$V(A,n;B,m) = \langle (x - R_A)^n (x - R_B)^m g_A^* g_B \rangle.$$

All matrix elements are expressed analytically and the  $X$  vector is easily obtained from Eq. (3.4) by inverting the complex matrix  $C$ . Since most standard integration routines require an expression for the time derivatives of each parameter, it is necessary to perform some simple manipulations on the  $X$  vector in order to isolate all time derivatives before a standard integration routine, here a Runge Kutta fifth order scheme, is adopted. Heller<sup>2</sup> has pointed out that the  $a_A$  terms in the first block of the  $X$  vector causes numerical difficulties and that the stability of the calculations is improved if  $a_A$  is replaced by the complex variables  $Q_A$  and  $Z_A$  defined by

$$a_A = 0.5 Q_A / Z_A, \quad (3.6a)$$

$$\dot{Z}_A = Q_A / \mu,$$

such that the equation

$$\dot{a}_A + 2a_A^2/\mu = (\text{right-hand side})$$

is replaced by two equations

$$\dot{Z}_A = Q_A / \mu, \quad (3.6b)$$

$$\dot{Q}_A = 2(\text{right-hand side}) Z_A.$$

This substitution is used in our calculations and increases the number of coupled differential equations from six to eight per wave packet.

To illustrate the relations between the MEM equations and the LHA equations let us consider just one wave packet. From Eq. (3.4) we find

$$\dot{R}_1 = P_1/\mu, \quad (3.7)$$

$$\dot{P}_1 = \frac{V(1,1;1,0)}{C(1,1;1,1)} = - \frac{\langle g_1 | \partial v / \partial x | g_1 \rangle}{\langle g_1 | g_1 \rangle},$$

$$\dot{a}_1 = -2a_1^2/\mu$$

$$+ \frac{C(1,2;1,0)V(1,0;1,0) - C(1,0;1,0)V(1,2;1,0)}{C(1,0;1,0)C(1,2;1,2) - C(1,2;1,0)C(1,2;1,0)},$$

$$\dot{\gamma}_1 = i\hbar a_1/\mu + P_1^2/2\mu$$

$$+ \frac{C(1,2;1,0)V(1,2;1,0) - C(1,2;1,2)V(1,0;1,0)}{C(1,0;1,0)C(1,2;1,2) - C(1,2;1,0)C(1,2;1,0)}$$

which shows that the equations of motion for the center of the wave packet are as given by Ehrenfest's theorem.<sup>16</sup> If the potential  $v(x)$  is expanded to second order in a Taylor series around  $R_1$ , we obtain Heller's equations of motion,<sup>2</sup> where the center of the GWP follows a classical trajectory. It is of interest to note that Heller implied the relation  $dR_1/dt = P_1/\mu$  and showed that a classical trajectory resulted, whereas the MEM gives this result directly.

The complete set of equations in Eq. (3.4) has not been used in practical calculations.<sup>11</sup> Various approximations are introduced to reduce the complexity of the equations and to eliminate a numerical problem. In the independent Gaussian

approximation (IGA) all coupling terms in  $C$  and  $V$  between different Gaussians are set to zero and each wave packet is propagated independently of the others following the equations of motion given in Eq. (3.7). Another way is to freeze the complex width parameters and not let them change in time. The relations between the various approximations and Heller's equations are discussed in detail in Ref. 10.

#### IV. THE STATIONARY STATES OF THE MORSE OSCILLATOR

Numerous ways have been used to determine the parameters of the Gaussian functions representing the initial stationary states to be propagated. We have found the method of Hamilton and Light<sup>8</sup> very useful because it is a good starting point in the development of a criteria for an accurate propagation using some of the approximations mentioned above. Since the method has not been used before in conjunction with the GWP approach and constitutes a good basis for the discussion in Sec. V, it is reviewed briefly.

The wave functions for the bound states are real and represented by a basis set of the form

$$\begin{aligned}\psi(x) &= \sum_{B=1}^N c_B g_B(x), \\ g_B(x) &= \exp\left[-\frac{1}{\hbar} \text{Im}(a_B)(x - R_B)^2\right], \\ c_B &= \exp\left[\frac{i}{\hbar} \text{Re}(\gamma_B)\right] \exp\left[-\frac{1}{\hbar} \text{Im}(\gamma_B)\right].\end{aligned}\quad (4.1)$$

The expansion coefficients  $c_B$  are determined by the well-known Rayleigh-Ritz variational method.<sup>16</sup> The complex exponent only determines the sign, that is,  $\text{Re}(\gamma_B)/\hbar = 0$  or  $\pi$ . The other parameters in Eq. (3.1) are zero for the initial state. A bound state wave function with quantum number  $n$  has  $n$  nodes and requires accordingly at least  $(n + 1)$  or more basis set functions  $g_B(x)$ , each characterized by two parameters  $\text{Im}(a_B)$  and  $R_B$ , to give the right number of nodes. The bound states are localized in space, and the turning points of the classical motion for a given energy are a good measure of the localization. A simple and direct way of choosing the positions and widths of the Gaussians would be to space them uniformly between the turning points for some energy and let the widths of the Gaussians be the distance between neighboring Gaussians. If all bound states are of interest, the turning points are chosen for an energy close to the dissociation energy for the potential. If however, only states up to a certain energy are of interest, the choice of the turning points is ambiguous. It will be natural to use an energy equal to or larger than the one specified, since the localization of the states becomes more pronounced as the energy drops. Hamilton and Light refined the method outlined above by noting that the distance between the nodes near the center of the Morse potential is smaller than in other regions reflecting the larger kinetic energy in the central region. Therefore, a better representation of the states is achieved if the Gaussians are spaced more densely in that region than in the outer regions. A semiclassical determination of the node positions may be obtained from the classical action integral<sup>17</sup>

$$\begin{aligned}n + \frac{1}{2} &= \frac{1}{\pi} \int_{x_-}^{x_+} dx \sqrt{[E_n - V(x)] 2m/\hbar^2} \\ &= M - \frac{1}{2},\end{aligned}\quad (4.2)$$

where  $x_-$ ,  $x_+$  are the left and right turning points of the classical motion for quantum state  $n$  with energy  $E_n$ .  $M$  is the minimum number of basis functions required ( $= n + 1$ ). The position  $x_1$  of the first Gaussian is chosen such that

$$\frac{1}{\pi} \int_{x_-}^{x_1} dx \cdots = \frac{1}{4}. \quad (4.3a)$$

The position  $x_2$  of the next Gaussian is chosen by

$$\frac{1}{\pi} \int_{x_1}^{x_2} dx \cdots = 1 \quad (4.3b)$$

and so on. When more than the minimum number of basis set functions are used, say  $N$ , the right-hand sides of Eq. (4.3) are just scaled by the factor  $(M - 0.5)/(N - 0.5)$ . The widths of the Gaussians are chosen from the expressions

$$\begin{aligned}\frac{\text{Im}(a_1)}{\hbar} &= \frac{C^2}{(x_2 - x_1)^2}, \\ \frac{\text{Im}(a_j)}{\hbar} &= \frac{C^2}{[(x_{j+1} - x_{j-1})/2]^2}, \quad 1 < j < N, \\ \frac{\text{Im}(a_N)}{\hbar} &= \frac{C^2}{(x_N - x_{N-1})^2},\end{aligned}\quad (4.4)$$

where  $C$  is a constant usually set to one. They are directly related to the distance between the centers of the Gaussians and chosen in that way to reduce the effect of overcrowding in the set.

Hamilton and Light have analyzed their results by comparing the calculated energies with the exact energies (2.6). They find that the best results for states up to a given quantum number  $n$  are obtained with a basis set, which has about twice the number of basis functions required distributed between the turning points of the classical motion for the energy of quantum state  $n$ . Addition of more Gaussians tends to reduce the accuracy due to the overcrowding and a reduction in the number of Gaussians also tends to reduce the accuracy due to an insufficient flexibility of the basis set. Another important finding is that the results are relatively insensitive to smaller changes in the position and width parameters. This is seen, for example, by comparing with the results based on the more primitive scheme outlined above, where the Gaussians are spaced uniformly between the turning points.

We have supplemented the investigations of the method to include the quality of the wave functions by calculating transition matrix elements of the types  $\langle n|x|m \rangle$  and  $\langle n|x^2|m \rangle$  and compare them with analytical results (2.9) and numerical integrations based on the analytical expressions for the wave functions. A Morse oscillator with  $\lambda = 10$  has been chosen for the comparisons and with a ground state energy of about 0.1 in the units used in Fig. 1, all states are seen to have a strong anharmonic character. In Table I the exact energies are compared with calculated energies using basis sets with, respectively, 10, 20, and 30 Gaussians. Since all ten bound states are of interest a minimum of ten Gaussians are required and the turning points are defined by the

TABLE I. The calculated energies of a Morse oscillator with  $\lambda = 10$  and with the Gaussian functions distributed between the turning points of the classical motion for the energy of the  $n = 9$  state. Results for different numbers,  $n_{\text{gaus}}$ , of basis functions are compared to the exact results.  $\Sigma\sigma^2$  is the sum of the squared difference between exact and calculated results.

$n$	$\epsilon_n$		$\epsilon_n$	
	exact	$n_{\text{gaus}} = 10$	$n_{\text{gaus}} = 20$	$n_{\text{gaus}} = 30$
0	9.750 00	9.780 54	9.751 70	9.750 50
1	27.750 0	27.782 3	27.752 4	27.752 4
2	43.750 0	43.922 6	43.756 0	43.757 4
3	57.750 0	58.802 1	57.762 5	57.767 2
4	69.750 0	72.212 4	69.770 8	69.781 4
5	79.750 0	83.354 3	79.776 9	79.795 8
6	87.750 0	91.718 9	87.779 3	87.804 6
7	93.750 0	97.230 1	93.778 2	93.802 9
8	97.750 0	99.825 3	97.786 2	97.790 8
9	99.750 0	109.968	99.781 5	99.805 1
$\Sigma\sigma^2$	...	156.57	5.31 - 03	1.39 - 02

energy of quantum state  $n = 9$ . At the bottom of the table the sum of the squared differences between exact and calculated energies is given and used as an indication of the overall agreement. The best results are obtained with a basis set of 20 Gaussians, which is twice the required number, and our findings are in agreement with Hamilton and Light. The results for the transition elements in Tables II and III show good agreement between the exact or numerical results and the results obtained with the 20 Gaussians supporting the general conclusions of Hamilton and Light. The deviations are usual much less than 1% and only for the small matrix elements, which are very sensitive to numerical errors, they become up to 5%. The pattern is the same for other matrix elements. The importance of the choice of turning points is illustrated by the results in Table IV, where the energy of quantum state  $n = 3$  has been used to define them. The basis set has eight Gaussians which is the minimum number for a representation of the first eight bound states. The situation for the first four bound states in Table IV is equivalent to the  $n_{\text{gaus}} = 20$  case in Table I, and we also note that the accura-

cy of the results are similar. For the upper four bound states the results are very poor also when compared to the  $n_{\text{gaus}} = 10$  case in Table I. The reason is that the lower bound states are more localized than the higher states, and with a basis set confined between the turning points for the energy of the  $n = 3$  state, the representation of the higher states becomes very poor. Similarly, the representation of the low quantum states becomes poor if a given number of basis functions are distributed between the turning points for an energy, which is much higher than the energy of those states.

Our extension of the work of Hamilton and Light consists in a variational determination of the eigenstates with some of the basis function parameters varying, like it is done in electron structure calculations. We have restricted ourselves to vary the  $C$  parameter in Eq. (4.4), which controls the width of the Gaussians. The results are presented in Table V where we have listed the energies calculated with the standard value of  $C$  ( $= 1$ ) and with the optimized value of  $C$  ( $= 0.211\ 95$ ). The smaller  $C$  means broader Gaussians with a larger overlap. As expected the overall agreement is improved, but the rather large change in  $C$  also emphasizes the relative insensitivity to changes in the basis set parameters. Since the improvements are not dramatic and unimportant for our analysis, we have used Hamilton and Light's method with  $C = 1$  in our computations.

## V. THE PROPAGATION OF THE STATIONARY STATES

It was noted in Sec. III that for each Gaussian in the basis set we have to solve eight coupled differential equations, and from the analysis in the preceding section it is evident that the number of equations even for the lowest bound states becomes rather large. The numerical problems are related to the inversion of the  $C$  matrix in Eq. (3.7) at each time step. Heather and Metiu<sup>18</sup> have already addressed that problem. They monitored the overlap matrix (the central block in the  $C$  matrix) and found that one of the eigenvalues became extremely small before the inversion failed and the computation stopped. This indicates that a linear dependence between the basis set functions develops during the propagation. We studied the problem in a calculation of a

TABLE II. Comparison of matrix elements  $\langle n|x|m \rangle$  for the  $\lambda = 10$  Morse oscillator. The analytical results are obtained from Eq. (2.9), and the numerical results are based on the analytic expressions for the wave function. The Gaussian wave packets are distributed between the turning points of the classical motion for the energy of the  $n = 9$  state. Results for the different number of basis functions,  $n_{\text{gaus}}$ , are shown.

$n$	$m$	Analytic	Numerical	GWP		
				$n_{\text{gaus}} = 10$	$n_{\text{gaus}} = 20$	$n_{\text{gaus}} = 30$
0	0	...	7.784 - 02	7.798 - 02	7.785 - 02	7.786 - 02
1	0	2.291 - 01	2.291 - 01	2.308 - 01	2.291 - 01	2.290 - 01
2	0	3.797 - 02	3.797 - 02	3.912 - 02	3.799 - 02	3.799 - 02
3	0	1.052 - 02	1.052 - 02	1.157 - 02	1.054 - 02	1.055 - 02
4	0	3.870 - 03	3.868 - 03	4.944 - 03	3.895 - 03	3.902 - 03
5	0	1.732 - 03	1.730 - 03	2.609 - 03	1.756 - 03	1.765 - 03
6	0	8.976 - 04	8.949 - 04	1.459 - 03	9.178 - 04	9.286 - 04
7	0	5.169 - 04	5.143 - 04	6.958 - 04	5.332 - 04	5.441 - 04
8	0	3.121 - 04	3.098 - 04	3.066 - 04	3.237 - 04	3.333 - 04

TABLE III. Comparison of matrix elements  $\langle n|x^2|m\rangle$  for the  $\lambda = 10$  Morse oscillator. The numerical results are based on the analytical expressions for the wave function. The Gaussian wave packets are distributed between the turning points of the classical motion for the energy of the  $n = 9$  state. Results for different number of basis functions,  $n_{\text{gaus}}$ , are shown.

$n$	$m$	Numerical	GWP		
			$n_{\text{gaus}} = 10$	$n_{\text{gaus}} = 20$	$n_{\text{gaus}} = 30$
0	0	6.010 - 02	6.114 - 02	6.010 - 02	6.010 - 02
1	0	6.111 - 02	6.018 - 02	6.112 - 02	6.115 - 02
2	0	6.134 - 02	6.087 - 02	6.113 - 02	6.128 - 02
3	0	2.630 - 02	3.472 - 02	2.620 - 02	2.617 - 02
4	0	1.170 - 02	1.093 - 02	1.173 - 02	1.171 - 02
5	0	5.855 - 03	5.536 - 03	5.888 - 03	5.882 - 03
6	0	3.253 - 03	2.768 - 03	3.287 - 03	3.289 - 03
7	0	1.959 - 03	9.105 - 04	1.988 - 03	1.996 - 03
8	0	1.214 - 03	8.739 - 05	1.237 - 03	1.245 - 03

$\lambda = 10$  Morse oscillator with four Gaussians in the basis set distributed between the turning points of the classical motion for the  $n = 3$  energy. The representations of the  $n = 0$  and  $n = 1$  states are, accordingly, accurate and less accurate for the  $n = 2$  and  $n = 3$  states. Each of the four states were propagated and the results are shown in Table VI. We have listed the time when the computations failed due to a singular inverse  $C$  matrix. It happened at different times for the first three bound states but not for the  $n = 3$  state even when the propagation was extended in time to the equivalent of four oscillation periods. The different behavior of the  $n = 3$  and the  $n = 0, 1, 2$  states is related to the number of Gaussians in the basis set. The  $n = 3$  state is represented by the minimum number of Gaussians and none of these become negligible during the propagation. The other states are represented by more than the minimum number of Gaussians, and during the propagation some of these may fit the wave function in such a way that others become negligible causing one or more of the rows in  $C$  to be zero. This poses a serious problem for the application of the MEM. On one hand, it is necessary to use a basis set with at least twice the minimum number of basis functions to get a good representation of a state. On the other hand, the propagation of states with more than the minimum number of basis functions runs into numerical problems sooner or later making it impossible, for

TABLE IV. The calculated energies of a Morse oscillator with  $\lambda = 10$  and with the Gaussian functions distributed between the turning points of the classical motion for the energy of the  $n = 3$  state. Results for eight Gaussians in the basis set are compared to the exact results.

$n$	$\epsilon_n$ exact	$\epsilon_n$ $n_{\text{gaus}} = 8$
0	9.750 00	9.752 12
1	27.750 0	27.766 2
2	43.750 0	43.790 2
3	57.750 0	57.929 5
4	69.750 0	71.594 7
5	79.750 0	90.144 5
6	87.750 0	119.365
7	93.750 0	171.148

TABLE V. The calculated energies of a Morse oscillator with  $\lambda = 10$  and with 20 Gaussians distributed between the turning points of the classical motion for the energy of the  $n = 9$  state. Results for an optimized value of  $C = 0.211\ 95$  are compared to the results for the chosen value of  $C = 1$ .  $\Sigma\sigma^2$  has the same meaning as in Table I.

$n$	$\epsilon_n$ exact	$\epsilon_n$ $C = 1.0$	$\epsilon_n$ $C = 0.211\ 95$
0	9.750 00	9.751 70	9.750 06
1	27.750 0	27.752 4	27.750 3
2	43.750 0	43.756 0	43.750 4
3	57.750 0	57.762 5	57.750 4
4	69.750 0	69.770 8	69.751 8
5	79.750 0	79.776 9	79.756 8
6	87.750 0	87.779 3	87.763 6
7	93.750 0	93.778 2	93.767 7
8	97.750 0	97.786 2	97.780 3
9	99.750 0	99.781 5	99.806 0
$\Sigma\sigma^2$	...	5.31 - 03	2.66 - 03

example, to study excitations of the oscillator. The primary importance of the MEM is that it gives an exact set of equations of motion for the parameters of the Gaussians and that all approximative methods may be understood as special cases of these equations.

Previous work by Heather and Metiu<sup>18</sup> indicated that couplings between packets can be important. However, their conclusions were based on a single specific Morse oscillator. It is therefore important for the practical applications of the wave packet method to analyze in a more systematic way the conditions for the approximative methods to be valid. We have focused on the IGA, since it is the least restrictive assumption, and developed a criteria which may be used to find those states of a given Morse oscillator that may be propagated with a reasonable accuracy by the IGA. The propagation is monitored by the norm of the state and the projection of the propagated state on the initial state. Since the quantum mechanical propagator is unitary, the former quantity is equal to one at all times for a proper propagation and the latter also equals one if the propagation is unitary and the representation of the state is accurate. Thus, deviations from one in the norm may be used to detect deficiencies in the propagation, whereas deviations from one in the projection indicate deficiencies in the representation of the state only when the propagation is unitary. In all our calculations with the complete MEM equations the norm is conserved

TABLE VI. The time  $\tau$  for a stop in the exact propagation of states  $n$  by the MEM due to a singular  $C^{-1}$  matrix in Eq. (3.4) for a  $\lambda = 10$  Morse oscillator with four Gaussians distributed between the turning points of the classical motion for the energy of the  $n = 3$  state. Only the propagation of the  $n = 3$  state never failed.  $\tau_h$  is the oscillation time for the corresponding harmonic oscillator.

State $n$	Stop time $\tau/\tau_h$
0	2.2
1	1.2
2	0.2
3	...



and equals one even for strongly anharmonic states showing that the propagation is very accurate.

Let us consider a basis set with  $N$  Gaussians. For wave packet  $A$  the expectation value of the energy is found to be

$$\begin{aligned}\epsilon_A &= P_A^2 + \frac{|a_A|^2}{\text{Im}(a_A)} \\ &\quad + \lambda^2 \{1 + \exp[-2R_A + 1/2 \text{Im}(a_A)] \\ &\quad - 2 \exp[-R_A + 1/8 \text{Im}(a_A)]\} \\ &= \epsilon_{A,\text{classical}} + \frac{|a_A|^2}{\text{Im}(a_A)}.\end{aligned}\quad (5.1)$$

The potential energy is averaged over the wave packet and is only strictly the Morse energy when  $\text{Im}(a_A) \rightarrow \infty$ , the classical limit. In the IGA each wave packet is propagated independently, and the energy  $\epsilon_A$  is conserved, whereas the classical energy is seen to vary because  $a_A$  varies. The center of the packet oscillates and is confined by the turning points of the classical motion determined by  $\epsilon_A$  and the width pulsates. When it increases [ $\text{Im}(a_A) \rightarrow 0$ ] energy leaks from the pure quantum energy [second term in Eq. (5.1)] into the classical energy, where it appears as kinetic and potential energy. Upon reduction of the width energy leaks the opposite way. At time  $t = 0$ ,  $P_A$  and  $\text{Re}(a_A)$  equal zero as discussed in the previous section and Eq. (5.1) reduces to

$$\begin{aligned}\epsilon_A &= \text{Im}(a_A) + \lambda^2 \{1 + \exp[-2R_A + 1/2 \text{Im}(a_A)] \\ &\quad - 2 \exp[-R_A + 1/8 \text{Im}(a_A)]\}.\end{aligned}\quad (5.2)$$

The total energy of each packet is easily determined from this expression once the position and width have been cho-

sen, and the results for a  $\lambda = 80$  Morse oscillator are shown in Table VII. For simplicity the Gaussians have been spaced uniformly between the turning points of the classical motion for a given energy, although the more sophisticated method by Hamilton and Light has been used in the actual calculations, but this difference is unimportant for the present analysis. It is seen that for a given set of turning points (given  $\epsilon/\lambda^2$ ) the wave packet energy increases as the number of Gaussians,  $n_{\text{gaus}}$ , is increased. This is expected from Eq. (5.2) since the width of the Gaussians decreases [ $\text{Im}(a_A)$  increases]. Also, for a given number of Gaussians, the energy of the outer wave packets increases as we change from one set of turning points to a new set at a higher energy. This simply reflects the higher potential energy. In Fig. 2 is shown

TABLE VII. The energies of the individual wave packets for a  $\lambda = 80$  Morse oscillator as a function of the number,  $n_{\text{gaus}}$ , of basis set functions, which are distributed uniformly between the turning points of the classical motion for two different energies.

Turning points based on the $\epsilon/\lambda^2$	Number of Gaussians $n_{\text{gaus}}$	Wave packet energy $\epsilon_A/\lambda^2$
0.04	4	0.0388
		0.0190
	6	0.0220
		0.0418
		0.0616
		0.0428
		0.0356
		0.0380
		0.0481
		0.0646
0.07	4	0.0490
		0.0146
	6	0.0216
		0.0560
		0.0662
		0.0328
		0.0213
		0.0269
		0.0452
		0.0732

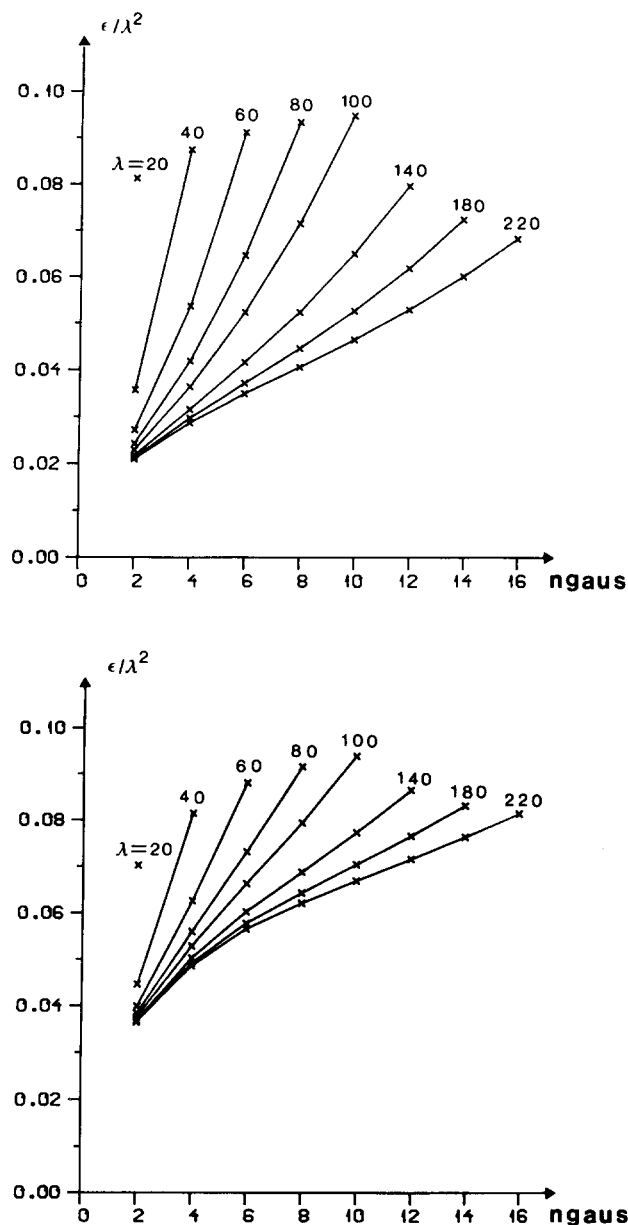


FIG. 2. The largest energy of a wave packet in a basis set as a function of the number,  $n_{\text{gaus}}$ , of wave packets, which are uniformly spaced between the turning points of the classical motion for an energy of, respectively,  $\epsilon/\lambda^2 = 0.04$  (a) and  $\epsilon/\lambda^2 = 0.07$  (b). The results for a series of Morse oscillators with different  $\lambda$  values are shown.

the maximum energy of a wave packet in a basis set as a function of the number of Gaussians in the set for a series of different Morse oscillators. The Gaussians are uniformly distributed between the turning points at the energies  $\epsilon/\lambda^2 = 0.04$  and  $0.07$ , respectively, and the widths are determined from Eq. (4.4) with  $C = 1$ . During the propagation the width of the Gaussians pulsates and as an extremum it may be infinite, and all the energy may be stored as potential energy. If this potential energy only differs slightly from the associated harmonic energy (Fig. 1) the IGA gives exact

results. Therefore, the IGA gives accurate results for states that are represented by a set of Gaussians, whose initial energies are in a region where the Morse potential is harmonic or nearly harmonic. Figure 1 may be used to estimate the maximum value of  $\epsilon/\lambda^2$ . Already at a value of  $0.1$  the difference between the Morse potential and the harmonic potential is considerable and by trial we have found that the energy should not be larger than about  $0.04$  to obtain an accuracy of a few percent. This conclusion is based on the results shown in Table VIII. We have considered a series of Morse oscilla-

TABLE VIII. The results of the IGA propagation of a series of different Morse oscillators  $\lambda$  and different states  $n$ . See the text for a further explanation.

$\lambda$	$n_{\text{gaus}}$	Max. $\epsilon/\lambda^2$ in the basis set [Fig. 2(a)]	State propagated $n$	$\Delta\epsilon_n$ (percent)	$\langle\Psi(t) \Psi(t)\rangle$ (percent)	Max. deviation in $ \langle\Psi(0) \Psi(t)\rangle ^2$ (percent)
20	2	0.080	0	3.4	20.5	12.5
	40	2	0	13.5	2.0	5.0
	4	0.088	0	5.0	70.0	20.5
			1	15.8	90.0	98.0
60	4	0.054	0	0.35	30.5	15.0
			1	2.2	20.0	40.5
80	4	0.042	0	0.01	10.5	5.0
			1	0.26	3.0	15.0
	6	0.065	0	0.3	60.5	20.5
			1	1.26	12.0	40.0
			2	5.35	70.0	80.0
100	4	0.036	0	0.19	3.0	2.0
			1	0.60	2.0	10.0
	6	0.053	0	0.05	20.05	12.5
			1	0.11	10.0	15.0
			2	1.16	15.5	40.0
140	4	0.032	0	0.70	0.0	0.0
			1	0.87	1.0	2.5
	6	0.042	0	0.47	5.0	3.5
			1	0.16	0.5	5.0
			2	0.47	0.0	16.0
	8	0.0525	0	0.44	25.0	12.0
			1	0.11	10.0	30.5
			2	0.26	7.0	25.0
	10	0.065	0	0.46	60.0	20.5
			1	0.18	11.0	50.0
			2	0.44	12.5	50.5
180	4	0.0295	0	2.97	0.0	0.1
	6	0.037	0	0.93	2.0	1.0
			1	0.10	1.0	2.0
			2	0.43	1.0	12.5
	8	0.045	0	0.89	10.0	5.5
			1	0.01	5.0	8.5
			2	0.02	2.5	14.0
	10	0.053	0	0.88	15.5	8.0
			1	0.01	8.5	20.5
			2	0.0	8.0	40.5
			3	0.28	10.5	40.0
220	4	0.028	0	6.79	0.0	2.0
			1	2.75	1.0	8.0
	6	0.035	0	0.99	0.0	0.0
			1	0.23	1.5	2.5
			2	0.5	3.0	10.0
	8	0.041	0	0.91	3.0	2.0
			1	0.03	1.0	8.0
			2	0.07	3.0	12.0
	10	0.047	0	0.90	10.0	8.5
			1	0.02	2.0	20.0
			2	0.04	3.5	25.5
			3	0.09	2.0	30.0

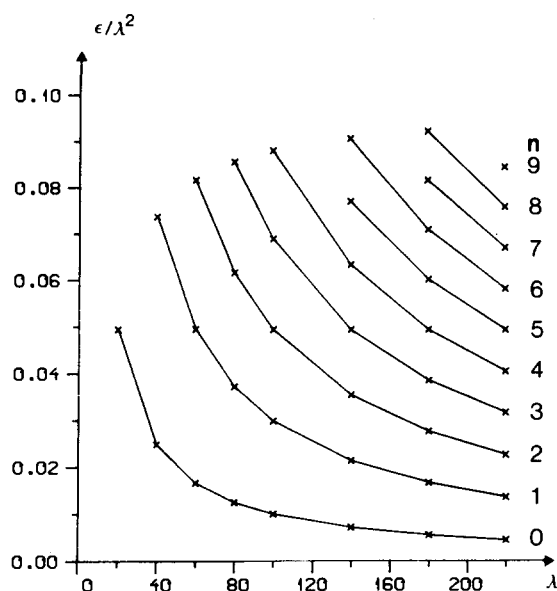


FIG. 3. The energies of the first bound states  $n$  of different Morse oscillators  $\lambda$ . The units are defined in Eqs. (2.3) and (2.5).

tors with  $\lambda$  values from 20 to 220 to cover a wide range of diatomic molecules. In the first column, the various  $\lambda$  values are listed. The number of Gaussian functions,  $n_{\text{gaus}}$ , is given in the next column and chosen under considerations of the conclusions in the previous section and in view of the energies of the individual Gaussians. The maximum energy of a wave packet in the given basis set (see Table VII) is listed in the third column and the states, which are propagated, are listed in column 4. The quality of the basis set is listed in column 5 as the deviation of the calculated energy from the theoretical energy for the various states in column 4. The results are given in the last columns, where the maximum deviation from one of the norm and the projection on the initial state has been recorded. All states were propagated for a time equal to four times the vibrational period of the corresponding harmonic oscillator. The table shows that the projections of the propagated state on the initial state are rather accurate for states which are well represented with the given basis set and propagated accurately.

## VI. SUMMARY

The time propagation of the stationary states of a Morse oscillator by the Gaussian wave packet method is very accurate, when the exact equations of motion as derived by the MEM, is used. Numerical problems, however, limits the utility of these equations severely. Only states represented by a basis set, which has just the minimum number of Gaussians necessary to give the correct number of nodes, are propagated without numerical problems. This number of basis functions is, however, too small for an accurate representation of the state, which requires about twice as many basis functions. There does not appear to be a simple way to get

around this problem, and it may be concluded that the MEM is difficult to apply in practical calculations. For harmonic potentials the IGA is exact, and for the Morse potential results with an accuracy of a few percent were obtained for states, which can be represented by Gaussians distributed between the turning points of the classical motion for an energy of 0.04 or smaller in the units on Fig. 1. The energies of the different stationary states of various Morse potentials are shown in Fig. 3 as a function of  $\lambda$ . The graph may be used to find those states which have an energy equal to or smaller than 0.04. For a  $\lambda = 100$  Morse potential it is only the ground state and the first excited state and for a  $\lambda = 200$  potential only the first three or four bound states. This is a very small fraction of the total number of bound states and a serious limitation in particular for processes where the excitation of the higher vibrational levels are important. The utility of the IGA is limited to processes, which only involves the first few bound states of the potential, and cannot be used in studies involving the higher vibrational states and dissociations. The calculations leading to the results in Table VIII were repeated with the widths of the Gaussians frozen (IFA) and the results were in general poorer due to the reduced flexibility of the basis set. This does not exclude the possibility of finding examples where the IFA leads to better results as reported by Skojde and Truhlar.<sup>11</sup> However, it is our finding that this is an exception rather than the rule. Thus, the primary importance of the Gaussian wave packet method seems to be that it offers a useful insight in the difference between classical and quantum dynamics and only in situations where the states are very localized or the process is very fast, it may be used in practical calculations unless other propagation schemes are developed.

## ACKNOWLEDGMENT

We wish to thank Professor J.P. Dahl, Department of Chemical Physics, The Technical University of Denmark, for his current interest in the work and for stimulating discussions.

- <sup>1</sup>E. J. Heller, J. Chem. Phys. **65**, 1289 (1976).
- <sup>2</sup>E. J. Heller, J. Chem. Phys. **62**, 1544 (1975); **64**, 63 (1976); **65**, 4974 (1976).
- <sup>3</sup>N. E. Henriksen, V. Engel, and R. Schinke, J. Chem. Phys. **86**, 6872 (1987).
- <sup>4</sup>N. E. Henriksen, G. D. Billing, and F. Y. Hansen, Chem. Phys. Lett. **149**, 397 (1988).
- <sup>5</sup>J. P. Chesick, J. Chem. Phys. **49**, 3772 (1968).
- <sup>6</sup>B. W. Shore, J. Chem. Phys. **59**, 6450 (1973).
- <sup>7</sup>M. J. Davis and E. J. Heller, J. Chem. Phys. **71**, 3383 (1979).
- <sup>8</sup>I. P. Hamilton and J. C. Light, J. Chem. Phys. **84**, 306 (1986).
- <sup>9</sup>K. C. Kulander and E. J. Heller, J. Chem. Phys. **69**, 2439 (1978); E. J. Heller, *ibid.* **68**, 2066, 3891 (1978); S. Y. Lee and E. J. Heller, *ibid.* **71**, 4777 (1979); R. C. Brown and E. J. Heller, *ibid.* **75**, 186 (1981); S. Y. Lee and E. J. Heller, *ibid.* **76**, 3035 (1982); G. Drolshagen and E. J. Heller, *ibid.* **79**, 2072 (1983); Surf. Sci. **139**, 260 (1984); R. Kosloff and C. Cerjan, J. Chem. Phys. **81**, 3722 (1984).
- <sup>10</sup>S. I. Sawada, R. Heather, B. Jackson, and H. Metiu, J. Chem. Phys. **83**, 3009 (1985).
- <sup>11</sup>R. T. Skojde and D. G. Truhlar, J. Chem. Phys. **80**, 3123 (1984); K. C. Kulander and A. E. Orel, *ibid.* **85**, 834 (1986); B. Jackson and H. Metiu, *ibid.* **84**, 3535 (1986).
- <sup>12</sup>P. M. Morse, Phys. Rev. **34**, 57 (1929).

- <sup>13</sup>M. M. Nieto and L. M. Simmons, Jr., *Phys. Rev. A* **19**, 438 (1979).
- <sup>14</sup>G. Herzberg, *Spectra of Diatomic Molecules* (Van Nostrand, New York, 1955).
- <sup>15</sup>V. S. Vasan and R. J. Cross, *J. Chem. Phys.* **78**, 3869 (1983); J. A. A. Gallas, *Phys. Rev. A* **21**, 1829 (1980); K. Scholz, *Z. Phys.* **78**, 751 (1932); J. E. Rosenthal, *Proc. Natl. Acad. Sci. U.S.A.* **21**, 281 (1935); L. Infeld and T. E. Hull, *Rev. Mod. Phys.* **23**, 21 (1951); H. S. Heaps and G. Herzberg, *Z. Phys.* **133**, 48 (1952).
- <sup>16</sup>L. I. Schiff, *Quantum Mechanics* (McGraw-Hill, New York, 1968).
- <sup>17</sup>H. Goldstein, *Classical Mechanics* (Addison-Wesley, Reading, MA, 1965).
- <sup>18</sup>R. Heather and H. Metiu, *J. Chem. Phys.* **84**, 3250 (1986).